# Interaction and charge transfer in the iron nitride $Fe_4N$

Wei Zhou, Li-jia Qu, and Qi-ming Zhang
*Institute of Physics, Academia Sinica, Beijing, China*

Ding-sheng Wang*
*Chinese Center of Advanced Science and Technology (World Laboratory), P.O. Box 8730, Beijing, China*
(Received 24 April 1989)

The linearized augmented-plane-wave method has been used to calculate the electronic bands of the cubic iron nitride $Fe_4N$. Strong interaction between N $2p$ and Fe $4s$ orbitals of nearest Fe atoms (Fe II) has been revealed. This interaction leads to an increase in the N $2p$ population. The Fe $3d$ bands remain almost the same as in the pure Fe metal with negligible interaction with neighboring N orbitals. However, the occupation of the Fe II $3d$ bands and the total number of electrons of Fe II atoms increases due to less screening. This unified picture clarifies the controversy in the previous explanations of the experimental results obtained from magnetic measurements, electron diffraction, and photoelectron spectroscopy.

## I. INTRODUCTION

In recent years, the metalloids consisting of transition-metal and some nonmetal elements with weak electron negativity, such as N, P, and B, are important subjects of research interest in the solid-state materials. The coexistence of interactions of the metal-metal atoms and the metal-nonmetal atoms provides a large variety of interesting physical phenomena and valuable properties, and thus has attracted a great deal of attention. From the theoretical point of view, the study of these materials is also a challenging problem: both localized $d$ and delocalized $s$ electrons of transition-metal elements and both the ionic and covalent character of those nonmetal elements with weak electron negativity have to be taken into account. Because of this complexity, the electronic configurations inferred from different experimental findings are often controversial. A unified picture is undoubtedly necessary for these metalloids.

Iron nitride is a typical example of these metalloids. The structure of the cubic $\gamma$-phase $Fe_4N$, hexagonal $\epsilon$-phase solid-solution $Fe_xN$ $(2<x<3)$, and tetragonal $\zeta$-phase $Fe_2N$ have been determined by Jack,[1] followed by the investigation of the magnetism,[2] electron and x-ray diffraction,[3] neutron diffraction,[4] Mössbauer[5] and photoelectron spectroscopy.[6] Electron configuration, charge transfer, and the explanation of related properties have been suggested by many authors based on the above experiments. For example the so-called donor model, first suggested by Wiener *et al.*,[7] is based on the fact that the magnetic moment of Fe atoms decreases with increasing number of its N neighbors when $x$ of $Fe_xN$ goes from 4 to 2. In the case of cubic $Fe_4N$ (Fig. 1), the N atom at the body center acts as the donor by giving three $2p$ electrons to its six nearest Fe neighbors at the face center (Fe II as shown in Fig. 1). Because each Fe II has two neighboring N atoms, the suggested configuration is $(\text{Fe I})^0(\text{Fe II})_3{}^{1-}\text{N}^{3+}$ for the cubic $Fe_4N$. Fe I denotes the Fe atom at the cubic corner position. It is not nearest to N, and is thus assumed to be in the neutral state. This configuration agrees with the neutron data[4] which give the magnetic moments of Fe I and Fe II atoms as $2.98\mu_B$

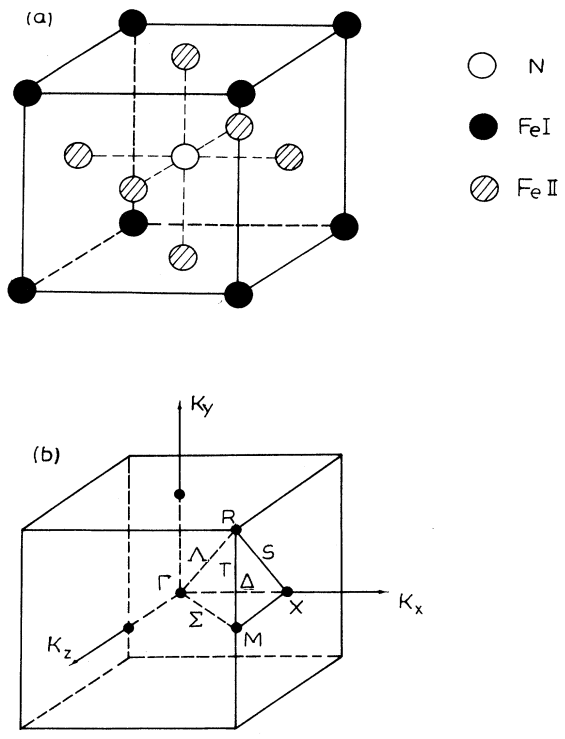


FIG. 1. (a) Unit cell of cubic $\gamma$-phase $Fe_4N$, $a=3.7946$ Å$=7.1707$ a.u. and (b) Brillouin zone and its $\frac{1}{48}$ irreducible wedge.

 

and $2.01\mu_B$, respectively, and also agrees with the measurement of Mössbauer hyperfine fields.[5]

However, Nagakura[3] has determined the form factor of the electron distribution of N atoms in the $Fe_4N$ by electron and x-ray diffraction. The result shows that the configuration of the N atoms is better described by $N^{1-}$, instead of the $N^{3+}$ configuration inferred from magnetic measurements of the Fe atoms. A configuration $(Fe\,I)^0(Fe\,II)_3{}^{1/3+}N^{1-}$ is thus assumed for the cubic $\gamma$-phase $Fe_4N$. Different from the above two descriptions, Ertl *et al.*[6] have reached a conclusion that there is no charge transfer between Fe and N atoms from their photoelectron spectroscopy results that the 3*d* bands show no change during nitrition.

Obviously, this controversy does not come from any inaccuracy of the above experiments, but has its origin in the fact that every measurement sees only one aspect of the electron configuration. In the present paper, we will report the results of a self-consistent band calculation for the cubic $Fe_4N$ by an *ab initio* linearized augmented-plane-wave (LAPW) method. A unified picture has been given for the interaction and charge transfer between N 2*p*, Fe 4*s*, and Fe 3*d* orbitals.

## II. METHODOLOGY

The highly accurate, linearized augmented-plane-wave method[8] is employed to carry out the calculation of the electronic structure of cubic $\gamma$-phase $Fe_4N$. This method has been generalized by several authors[9] by considering core electrons in self-consistency, treating more general potentials (warped muffin-tin), and including relativistic effects, the core states (Fe 1*s* through 3*p* and N 1*s*) are computed self-consistently for every iteration using a fully relativistic Dirac-Slater-type atomic-structure program. The valence states (Fe 3*d* and 4*s*, and N 2*s* and 2*p*) are computed semirelativistically, i.e., the Dirac equation is solved with mass-velocity and Darwin terms included, but without the spin-orbital coupling. A Coulomb contribution to the potential is obtained by an accurate solution of Poisson's equation.

The exchange correlation takes the form of the local-density-functional approximation. The muffin-tin radius is set equal to 2.2 a.u. for Fe atoms for easy comparison with a previous calculation of Fe metal. The N muffin-tin radius is 1.38 a.u. in contact with Fe muffin-tin spheres. Four special $\bar{k}$ points in the $\frac{1}{48}$ irreducible Brillouin zone of the cubic cell are used to generate electron density and potential.[10] The basis size used in the eigenvalue problem is about 180 LAPW's. The convergency is assumed when the rms difference between the input and output potential is better than 30 mRy.

## III. ENERGY BAND AND DENSITY OF STATES

Along the high-symmetry lines of the first Brillouin zone [Fig. 1(b)], the calculated energy band is shown in Fig. 2. The lowest N 2*s* band is located between $-15.9$ to $-17.2$ eV below the Fermi energy. The interaction between N 2*s* and neighboring Fe II 4*s* orbitals is only $-0.006$ Ry as obtained by fitting this calculated energy band to a Slater-Koster-type description.[11] The strongest interaction is found for N 2*p* and neighboring Fe II 4*s* orbitals as can be seen from the hybridized bands from about $E=-4$ to $-7$ eV. Because at the $\Gamma$ point N 2*p* does not mix with Fe 4*s* states due to symmetry considerations, $\Gamma_1$ ($E=-6.26$ eV) and $\Gamma_{15}$ ($E=-4.38$ eV) are almost pure Fe 4*s* and N 2*p* states, respectively. However, this interaction manifests itself at *X*, *M*, and *R* points, where one, two, and three N 2*p* orbitals hybridize with neighboring Fe II 4*s* orbitals, respectively. The horizontal bands at $E=-7$ eV from *X* to *M* to *R* in Fig. 2 and the singlet (at *X*), doublet (at *M*), and the triplet (at *R*) show this hybridization. A contour plot of the single-particle charge density of the triplet at the *R* point ($E=-7.13$ eV) is depicted in Fig. 3 to show the strong bonding character. Because all three N 2*p* states are involved in this bonding, the charge density around the N atom is almost spherically symmetric except for the obvious bonding enhancement along the lines toward neighboring Fe II atoms. The Slater-Koster parameter from a least-squares fitting is $Vsp$ (Fe II,N)$=0.113$ Ry.[11]

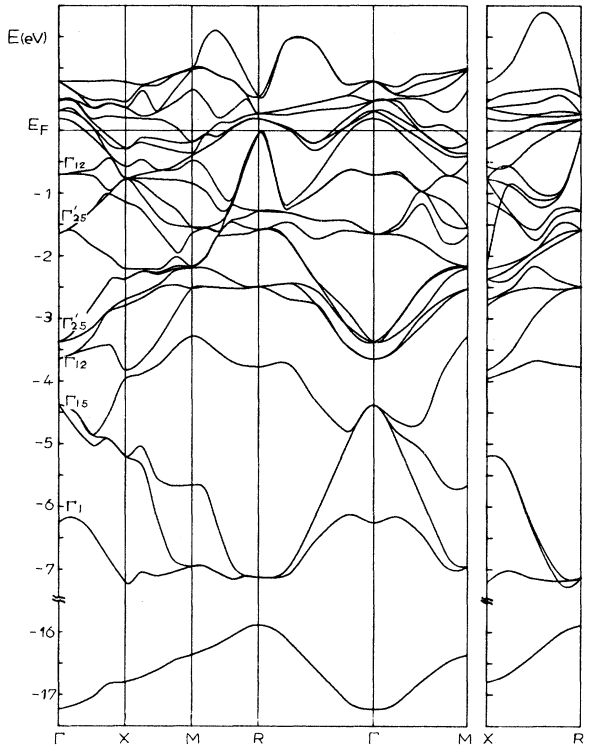


FIG. 2. Energy band of cubic $\gamma$-phase $Fe_4N$.

The interaction between N 2*p* and Fe 3*d* orbitals is negligibly small over most parts of the Brillouin zone except near the line from *X* to *M* (Fig. 2). The Fe 3*d* band is above $-4$ eV. With negligible interaction with the metalloid element, this *d* band is similar to that of the metal Fe.

The density-of-states (DOS) curve obtained by analytic tetrahedron interpolation[12] is given in Fig. 4. The Fe 3*d* band shows the typical character of metallic Fe. There

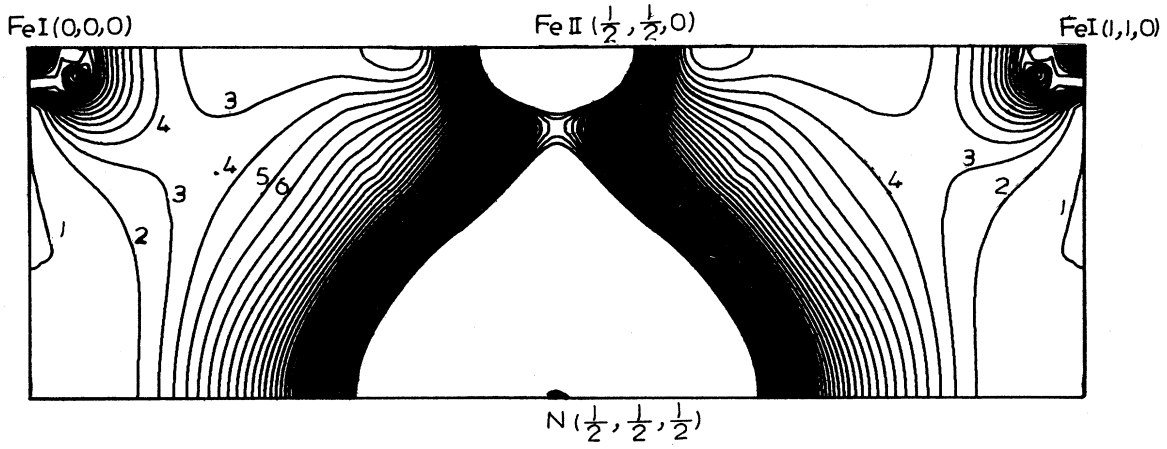


FIG. 3. Contour plot of the single-particle electron density at the $R$ point and $E = -7.13$ eV on a (110) plane through N, Fe I, and Fe II atoms. Electron density is shown in units of 0.001 a.u.$^{-3}$

are three main peaks and the Fermi energy lies near the center of the highest-energy peak.[13] However, four additional peaks appear at $E = -7.0$, $-5.7$, $-4.6$, and $-3.7$ eV corresponding to N $2p$–Fe II $4s$ bonding, Fe $4s$ nonbonding, N $2p$ nonbonding, and N $2p$–Fe II $4s$ antibonding states, respectively. This feature could be revealed by an inspection of the energy band shown in Fig. 2.

This result agrees with the photoelectron measurement in Ertl *et al.*[6] During nitrition, no change happens in the Fe $3d$ bands from the Fermi energy down to $-3.5$ eV according to their results, but two broad bumps could be seen from $-3.5$ to $-5.3$ eV and $-5.3$ to $-8.0$ eV on the experimental curve (curve $C$ in Fig. 5 of Ref. 6). By a careful study, the two bumps could be identified as four peaks at $-7.5$, $-6.2$, $-4.7$, and $-4.0$ eV. Though the experiment is carried out during the nitrition process of ion implantation, the N contribution is in good agreement with the present calculation of cubic $Fe_4N$. This agreement is evidence of the strong local interaction between N $2p$ and its neighboring Fe $4s$ orbitals and shows that the Fe $3d$ orbitals do not interact with N orbitals, although this does not imply that the Fe $3d$ occupation may not change, as suggested by Ertl *et al* in Ref. 6, for the reasons explained in the following sections.

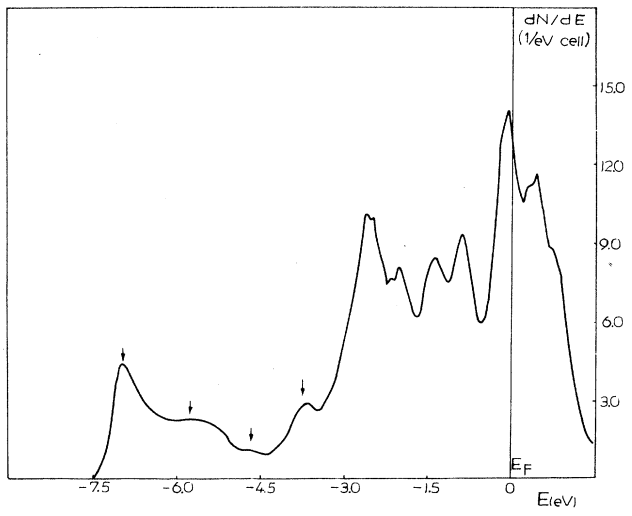


FIG. 4. Density of states of cubic $\gamma$-phase $Fe_4N$.

## IV. TOTAL ELECTRON DENSITY AND CHARGE TRANSFER

The total electron density is plotted on a (110) plane containing N, Fe II, and Fe I atoms (Fig. 5). The nonspherical part of the electron density inside the muffin-tin sphere is expanded in terms of the lattice harmonics from 1 up to 6.

Around the N core, the radius of the electron sphere is about 2.28 a.u. (arrow $A$ in Fig. 5). It is much larger than the atomic radius of a neutral atom (1.7 a.u.), indicating a negative ion configuration. Taking the radial electron density along line $A$ in Fig. 5 and assuming a spherical distribution as shown in the contour plot, the total integrated number of valence electrons within that sphere (radius 2.28 a.u.) is 6.08, i.e., 1.08 more than neutral N atom. This result agrees with Nagakura,[3] who has shown that the $N^{1-}$ configuration gives a best fit to the electron and x-ray-diffraction data. However, this does not necessarily mean that the neighboring Fe II atoms should lose electrons to the N atom and be in a positive Fe II configuration. Compare the electron distribution of Fe II and Fe I atoms. The electron density minimum on the line connecting Fe II to the N center is 0.11 a.u.$^{-3}$ and the length of line $C$ (Fig. 5) is 1.78 a.u. The contour of the same electron density around the Fe I atom is smaller as shown by line $D$ (1.58 a.u.). This difference is also shown in Table I, which compares the electron number within the muffin-tin region and its angular momentum decomposition for Fe I and Fe II.

TABLE I. Total number of electrons in the muffin-tin sphere ($R=2.20$ a.u.) of Fe I and Fe II atoms in cubic $Fe_4N$ and their $l$ decomposition.

| | Total | $s$ | $p$ | $d$ |
|---|---|---|---|---|
| Fe I | 6.44 | 0.28 | 0.23 | 5.92 |
| Fe II | 6.78 | 0.29 | 0.34 | 6.10 |

It is obvious that Fe II atoms have 0.34 more electrons than Fe I atoms due mainly to more occupation of $d$ orbitals. Though we have not made a spin-polarized calculation, the above result already enables us to make a comparison with magnetic measurements. As it is well known, the increase in the total electron number will lead to a decrease in magnetic moments for such elements as Fe, Co, and Ni with a nearly filled $d$ band. The decrease of magnetic moments is, according to calculations for other systems (for example in Ref. 14), equal to the increase in the number of total electrons. So the increase of 0.34 electrons of Fe II atoms over that of Fe I as given by the present calculation is, at least, in qualitative agreement with the neutron diffraction result[4] that the magnetic moment of Fe II atoms is $0.97\mu_B$ less than that of Fe I atoms. The quantitative difference could be presumably improved in a spin-polarized calculation, since the exchange splitting will push the minority-spin band further up. It is also in qualitative agreement with the donor model in the description of the dependence of the electron number of Fe atoms with its N neighbors. However, according to the present calculation the increase of Fe II electrons is certainly not from a donation by N $2p$.

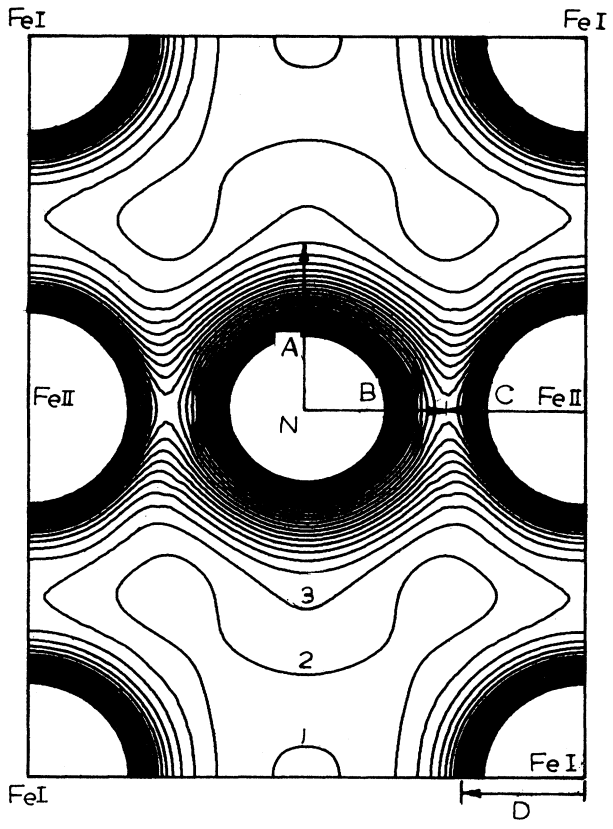


FIG. 5. Total charge density on a (110) plane through N, Fe I, and Fe II atoms. The contours are shown in units of 0.01 a.u.$^{-3}$. The characteristic lengths $A=2.28$ a.u., $B=1.81$ a.u., $C=1.78$ a.u., and $D=1.56$ a.u. (for discussion see text).

So we have already succeeded in giving a unified picture which agrees with the magnetic-electron- and x-ray-diffraction and photoelectron-spectroscopy measurements. The problem or the missing part in previous discussions is the neglect of the essential role of the Fe II $4s$ electron, i.e., both its interaction with the N $2p$ orbitals and its influence on Fe II $3d$ occupation. The interaction between Fe II $4s$ and N $2p$ orbitals makes strong bonding, and part of the $4s$ electron, especially that in the interstitial region, thus changes its spatial distribution and fills the N $2p$ states. This change moves the Fe II $4s$ electron toward the Fe-N bonding region, and leads to less screening of the Fe II $3d$ electron from the nuclear attraction. This outward shift of the Fe II $4s$ electron to the Fe-N bonding region is not indicated in Table I, which gives the same number of $s$ components of Fe I and Fe II atoms because the muffin-tin radius of Fe atoms $R=2.20$ a.u. is so large that the bonding region is also included in that muffin-tin sphere, but it is clearly seen in the following section from core-level shifts. This decrease in screening lowers the Fe II $3d$ bands so that the bottom of the Fe $3d$ bands ($\Gamma_{12}$ and $\Gamma_{25}$ in Fig. 2) is only 2–3 eV above the bottom of the Fe $4s$ band ($\Gamma_1$ in Fig. 2). The corresponding difference is 6 eV for metallic iron.[13] Due to this effect the Fe II $3d$ occupation is increased during nitrition, though the Fe II $3d$ orbitals do not interact with N $2p$ as shown in Fig. 2 by the band calculation or by photoelectron measurements. This consideration is believed to be quite general in discussing the electronic configuration of an interacting system consisting of transition-metal elements and other atoms. For example, by comparing the interaction of H with Ni to that of H with Cu, Harris and Andersson[15] have already described the same mechanism that lifted the Ni $4s$ orbital due to its interaction with the H orbital and the Ni $3d$ bands act as a basin to accept electrons from the lifted $4s$ states.

## V. CORE-LEVEL AND ISOMER SHIFT

Table II gives the calculated results of the core levels. As discussed in the previous section, the Fe-N bonding leads to the shift of the Fe II $4s$ electron to the bonding area and less screening of other electrons on inner orbits. Levels $1s$, $2s$, and $2p$ of Fe II atoms shift about 0.8 eV as compared to that of Fe I, and levels $3s$ and $3p$ shift 0.5 eV to the higher binding energy as given in Table II. Ertl *et al.*[6] have observed that the Fe $3p$ level shifts to slightly higher binding energy during nitrition, but it is hard to make a quantitative comparison due to the poor resolution of that measurement. Table III lists the electron density of Fe I and Fe II atoms at their nuclear sites (contact density) for $s$ and $p_{1/2}$ orbitals. In comparison, the contact density for the metal Fe is also listed, taken from

TABLE II. Core levels of Fe I and Fe II atoms in cubic $Fe_4N$ (reference to Fermi energy), and the difference between the corresponding levels of Fe I and Fe II atoms.

| | Fe I (Ry) | Fe II (Ry) | $\Delta E$ (Ry) | $\Delta E$ (eV) |
|---|---|---|---|---|
| $1s$ | −511.875 | −511.920 | 0.063 | 0.86 |
| $2s$ | −58.839 | −58.891 | 0.052 | 0.71 |
| $2p_{1/2}$ | −50.628 | −50.682 | 0.054 | 0.75 |
| $2p_{3/2}$ | −49.714 | −47.768 | 0.054 | 0.75 |
| $3s$ | −5.622 | −5.697 | 0.035 | 0.48 |
| $3p_{1/2}$ | −3.271 | −3.306 | 0.035 | 0.48 |
| $3p_{3/2}$ | −3.156 | −3.192 | 0.036 | 0.49 |

TABLE III. Contact density of electrons of Fe I and Fe II atoms in cubic $Fe_4N$ in a.u.$^{-3}$, and the isomer shift ($\Delta v$) with respect to metal Fe in mm sec$^{-1}$ a.u.$^3$.

| | Fe I | Fe II | Metal Fe (Ref. 13) |
|---|---|---|---|
| $1s$ | 13 301.58 | 13 301.64 | 13 300.86 |
| $2s$ | 1246.03 | 1246.28 | 1246.77 |
| $2p_{1/2}$ | 6.86 | 6.82 | 6.82 |
| $3s$ | 182.28 | 182.27 | 182.67 |
| $4s$ | 5.67 | 5.76 | 6.72 |
| Total $\rho$ | 14 743.38 | 14 743.72 | 14 744.79 |
| Total $\Delta\rho$ | −1.41 | −1.07 | 0 |
| $\Delta v$ | | | |
| Calc. | 0.37 | 0.28 | |
| Expt. (Ref. 16) | 0.24 | 0.31 | |

Ref. 13. A decrease of the contact density is shown for both Fe I and Fe II atoms, but the contribution from different shells is quite different. A decrease of about 14–16 % in the delocalized $4s$ component is easy to understand from the increase of the volume. For metal Fe ($a=5.417$ a.u.) the volume of each metal atom is 79.48 a.u.,$^3$ but for $Fe_4N$ it is 92.18 a.u.,$^3$ which shows just a 16% increase. Such variation in a $4s$ component is in coincidence with what happens during a volume contraction of the simple metal.[13] However, for a simple metal, the contributions from the inner $1s$, $2s$, and $3s$ electrons to the contact-density variation are opposite to that of the $4s$ electron showing the screening effect, and the total amount is only 30% of that of the $4s$ contribution. In the present case of $Fe_4N$, the contributions of $1s$, $2s$, and $3s$ electrons are stronger and different in sign. This is believed to be caused by a competing effect of the opposite variations of $4s$ and $3d$ occupation. The calculated total variations of the contact density of Fe I and Fe II atoms are −1.41 and −1.07 a.u.$^{-3}$, respectively. Taking the isomer-shift calibration constant −0.26 mm sec$^{-1}$ a.u.$^3$ from Ref. 13, the theoretical values of the isomer shift are 0.37 and 0.28 mm sec$^{-1}$ for Fe I and Fe II atoms. This result agrees with the experimental Mössbauer measurement by Nozik *et al.*[16] as shown in the last row of Table III.

## VI. CONCLUSIONS

It is shown that in the discussion of the electronic structure of the metalloids containing transition-metal elements, the interaction of the $4s$ and $3d$ electrons of the transition elements should be clearly distinguished. As shown in the present case of the Fe—N bonding, the interaction between N $2p$ and its neighboring Fe $4s$ is the strongest and determines the main features of the spatial electronic distribution, e.g., the form factor, given by the electron diffraction and the energy distribution given by the photoelectron spectroscopy. The direct interaction between the N $2p$ orbital and the localized Fe $3d$ states is weak even when they are neighboring to each other. However, both the energy with respect to the $4s$ level and the occupation of Fe $3d$ states have been changed due to the intra-atomic interaction, when the Fe $4s$ electron makes bonds with N $2p$ orbitals and redistributes itself. This picture gives a correct explanation to the magnetic properties of these metalloids. The long-standing controversy, which is seen to originate from considering only the direct electron transfer between Fe $3d$ and N $2p$ states and by neglect of the effect of the Fe $4s$ electron, has been clarified according to this unified picture.

## ACKNOWLEDGMENTS

This work is supported by National Science Foundation of China (NSFC) through Grant No. A84W17. Two authors (W.Z. and L.-J.Q.) wish to express their sincere thanks to Professor M. G. Zhao and Professor K. Fang of Sichuan Normal University.

*Mailing address: Institute of Physics, Academia Sinica, Beijing, China.

[1]K. H. Jack, Proc. R. Soc. London, Ser. A **34**, 195 (1947).
[2]Eickel *et al.*, Phys. Status Solidi **39**, 121 (1970); G. M. Chen *et al.*, J. Phys. Chem. **87**, 5326 (1983).
[3]S. Nagakura, J. Phys. Soc. Jpn. **25**, 488 (1968).
[4]B. C. Frazer, Phys. Rev. **112**, 751 (1958).
[5]G. M. Chen *et al.*, J. Phys. Chem. **87**, 5326 (1983).
[6]G. Ertl, M. Huber, and N. Thiele, Z. Naturforsch. A **34**, 30 (1979).
[7]G. W. Wiener and J. A. Berger, J. Met. **7**, 360 (1955).
[8]D. D. Koelling and G. O. Arbman, J. Phys. F **5**, 2041 (1975).
[9]M. Posternak, H. Krakauer, A. J. Freeman, and D. D. Koelling, Phys. Rev. B **21**, 5601 (1980).
[10]D. J. Chadi and M. L. Cohen, Phys. Rev. B **8**, 5747 (1973).
[11]L. Qu, M.S. thesis, Sichuan Normal University, 1987.
[12]J. Rath and A. J. Freeman, Phys. Rev. B **11**, 2019 (1975).
[13]Q. M. Zhang, Y. L. Zhang, and D. S. Wang, Commun. Theor. Phys. **8**, 139 (1987).
[14]D. S. Wang, A. J. Freeman, and H. Krakauer, Phys. Rev. B **26**, 1340 (1982).
[15]J. Harris and S. Andersson, Phys. Rev. Lett. **55**, 1583 (1985).
[16]A. J. Nozik, Solid State Commun. **8**, R8 (1970).